

Original Article:

Tibiofemoral Contact Forces in the Anterior Cruciate Ligament Reconstructed Knee

Authors: David J. Saxby¹, Adam L. Bryant⁴, Luca Modenese^{1,3,4}, Pauline Gerus², Bryce Killen¹, Jason Konrath¹, Karine Fortin⁵, Tim V. Wrigley⁵, Kim L. Bennell⁵, Flavia M. Cicuttini⁶, Christopher Vertullo^{7,1}, Julian A. Feller^{8,9}, Tim Whitehead⁸, Price Gallie¹⁰, David G. Lloyd¹

Affiliations: ¹Centre for Musculoskeletal Research, Menzies Health Institute Queensland, Griffith University, Gold Coast, Australia

²Laboratory of Human Motion, Education and Health, University of Nice Sophia-Antipolis, Nice, France

³INSIGNEO institute for *in silico* medicine, University of Sheffield, UK

⁴Department of Mechanical Engineering, University of Sheffield, UK

⁵Centre for Health, Exercise and Sports Medicine, University of Melbourne, Australia

⁶Department of Epidemiology and Preventive Medicine, Monash University, Australia

⁷Knee Research Australia, Australia

⁸OrthoSport Victoria, Epworth Richmond, Melbourne, Australia

⁹College of Science, Health and Engineering, La Trobe University, Melbourne, Australia

¹⁰Pacific Private Clinic, Gold Coast, Australia

Keywords: knee contact; ACL reconstructed gait; musculoskeletal modelling; EMG-driven modelling

Corresponding author: David John Saxby.

david.saxby@griffithuni.edu.au

+61755527066 (Phone), +61755528674 (Fax)

Abstract

Purpose: To investigate differences in ACL reconstructed (ACLR) and healthy individuals in terms of the magnitude of the tibiofemoral contact forces, as well as the relative muscle and external load contributions to those contact forces, during walking, running and sidestepping gait tasks.

Methods: A computational electromyography-driven neuromusculoskeletal model was used to estimate the muscle and tibiofemoral contact forces in those with combined *semitendinosus* and *gracilis* tendon autograft ACLR (n=104, 29.7±6.5 years, 78.1±14.4 kg) and healthy controls (n=60, 27.5±5.4 years, 67.8±14.0 kg) during walking (1.4±0.2 m·s⁻¹), running (4.5±0.5 m·s⁻¹) and sidestepping (3.7±0.6 m·s⁻¹). Within the computational model, the *semitendinosus* of ACLR participants was adjusted to account for literature reported strength deficits and morphological changes subsequent to autograft harvesting.

Results: ACLRs had smaller maximum total and medial tibiofemoral contact forces (~80% of control values, scaled to bodyweight) during the different gait tasks. Compared to controls, ACLRs were found to have a smaller maximum knee flexion moment, which explained the smaller tibiofemoral contact forces. Similarly, compared to controls, ACLRs had both a smaller maximum knee flexion angle and knee flexion excursion during running and sidestepping, which may have concentrated the articular contact forces to smaller areas within the tibiofemoral joint. Mean relative muscle and external load contributions to the tibiofemoral contact forces were not significantly different between ACLRs and controls.

Conclusion: ACLRs had lower bodyweight-scaled tibiofemoral contact forces during walking, running and sidestepping, likely due to lower knee flexion moments and straighter knee during

the different gait tasks. The relative contributions of muscles and external loads to the contact forces were equivalent between groups.

Introduction

Osteoarthritis (OA) is a prevalent degenerative joint disease that substantially burdens individuals and health care systems worldwide. The medial tibiofemoral (MTF) compartment of the knee is most commonly afflicted by OA (41), and knee loading during ambulation is considered to be a principal cause of the disease (1).

Individuals who have sustained anterior cruciate ligament (ACL) rupture and subsequent reconstruction (ACLR) are at significant risk for future onset of knee OA (3). The lasting effects of ACLR on an individual's knee biomechanics, as well as their muscle activation patterns, morphologies and strengths, may influence subsequent knee OA risk. During walking, ACLR individuals have a smaller knee flexion angle and moment (39), an increased knee adduction moment (9), and reduced *vasti* activation (6). Moreover, the donor muscles from which the ACL autograft is harvested subsequently experience fatty infiltration (40), atrophy (8, 40) and muscle-belly retraction (50). Following *semitendinosus* and *gracilis* ACLR, significant strength deficits in knee internal rotation (2) and flexion (8) have been reported, which is understandable as the impaired donor muscles were important knee internal rotators and flexors. Given muscle's role in loading the articulations of the knee (33), altered muscle activation patterns, morphologies and strengths, in addition to altered knee biomechanics following ACLR may considerably affect the tibiofemoral contact forces.

The tibiofemoral contact forces following ACLR have received limited research focus (16, 26, 42, 49). This scarcity of research may, in part, be due to the challenges of non-invasively determining muscle and tibiofemoral contact forces while accounting for altered gait biomechanics, abnormal muscle activation patterns and impairment of the donor muscles. Electromyography (EMG)-driven neuromusculoskeletal models may overcome these challenges by using non-invasive measurements of an individual's anatomy, external joint

biomechanics and muscle activation patterns to estimate muscle forces and moments (25) as well as tibiofemoral contact forces (17, 51). Notably, all of the previous investigations into ACLR tibiofemoral contact forces (16, 26, 42, 49) have used EMG-driven neuromusculoskeletal models.

Importantly, the ACLR knee has been shown to experience lower walking tibiofemoral contact forces compared to the unaffected contralateral knee at 6-months post-ACLR (49). Moreover, those ACLR individuals who developed radiographic medial knee OA by 5-years post-operation had significantly lower MTF contact forces in their ACLR knee at 6-months post-operation, while those who did not develop knee OA had symmetrical loading at 6-months post-operation (49). However, it remains unclear whether the ~20% BW reduction in the MTF contact forces in the ACLR knee (49) were sufficient to have caused the subsequent onset of knee OA, or whether the disease was due to the initial ACL injury, or some other unknown factor.

The aim of this study was to investigate possible differences in the tibiofemoral contact forces, and the relative contribution made by muscle and external loads to those contact forces, in ACLR individuals compared to healthy controls. Previous studies (16, 26, 42, 49) of ACLR tibiofemoral contact forces have analysed primarily walking gait, as it is the most common mode of human ambulation and therefore is a major determinant of the habitual mechanical environment of the knee's articular tissues. In this study we included walking gait, but also examined the more demanding gait tasks of running and sidestepping. Our rationale was that if the knee muscles were impaired (*i.e.* weaker with altered activation patterns) following ACLR as the literature indicates, we expected to see the influence of this impairment on the tibiofemoral contact forces during running and sidestepping because these tasks require significantly greater muscle activation than walking. Although ACLR individuals have reduced

knee muscle strength (2), an increased external knee adduction moment (eKAM) during walking (9) may increase the magnitude of the MTF contact forces or alter the medial-to-lateral distribution of the contact forces loading. Thus, our first hypothesis was that ACLR individuals will have larger tibiofemoral contact forces compared to healthy controls particularly during walking, but potentially during the other gait tasks as well. Our second hypothesis was that, because of the larger eKAM during walking (9), ACLR individuals would have greater relative proportion of the MTF contact forces generated by external loads (*i.e.* the net external frontal plane moment about the lateral tibiofemoral compartment) and a smaller relative contribution made by muscle compared to healthy controls during walking gait and potentially the other gait tasks.

Methods

This study was conducted at Griffith University's Centre for Musculoskeletal Research (CMR) and University of Melbourne's Centre for Health, Exercise and Sports Medicine (CHESM), approved by both Universities' human research ethics committees (CMR: PES/36/10/HREC, CHESM: 0932864.3) and data were equally acquired by the two institutions. All participants provided their written informed consent prior to testing, were 18-42 years of age and free of neuromusculoskeletal and cardiovascular diseases, had body mass indices $\leq 34 \text{ kg}\cdot\text{m}^{-2}$ and no self- or clinician-diagnosed OA. The study design was cross-sectional with participants either an ACLR individual (n=104, 55 and 49 tested at CHESM at CMR, respectively) or healthy control (n=60, tested equally between institutions) (Table 1 describes participant characteristics). Using data from Tsai et al (42), the estimated effect size of ACLR and healthy control tibiofemoral contact forces was large (Cohen's $d > 1$). The current investigation had an estimated 99% power to detect group differences in the tibiofemoral contact forces between ACLR and controls with an alpha of 0.05.

ACLRs were tested 2-3 years following ipsilateral *semitendinosus* and *gracilis* tendon autograft reconstruction performed ≤ 6 months after ACL rupture. Reconstructions were performed by one of four experienced orthopaedic surgeons. Semitendinosus and gracilis tendons were harvested using a 3-4 cm incision over *pes anserinus*. Excised sections were inter-wound, suspensory femoral fixation was achieved using an appropriate length Closed-Loop Endobutton (Smith and Nephew Endoscopy, Mass, USA), and an interference screw established graft-tibia mechanical fixation. Meniscal repair was undertaken if the surgeon judged the lesion repairable, and if a meniscal lesion was judged un-repairable and likely to be symptomatic, it was resected.

Each participant completed a gait analysis session wherein three-dimensional motion capture, ground reaction forces (GRFs) and EMGs were concurrently acquired during walking at self-selected pace, running at 4-5 m·s⁻¹ and running followed by 45° diagonal sidestepping (referred to in this study as “sidestepping”). Participants were allowed to warm-up by familiarizing themselves with each movement until they felt comfortable. For running, after each trial speed was assessed and verbal feedback provided to ensure participants ran ~ 4.5 m·s⁻¹. For sidestepping, participants were asked to execute the movement as fast as they felt they could safely perform the movement. Participants wore standardized footwear (<http://www.volley.com.au/>) and a full-body marker set with 10-marker clusters on thighs and shanks (12). A 10 (CMR) or 12 (CHESM) camera motion capture system (Vicon, Oxford Metrics Group, UK) acquired 3-dimensional marker trajectories (200 or 120 Hz, respectively). GRFs were acquired using two (CMR) (Kistler Instrumente, Switzerland) or three (CHESM) (Advanced Mechanical Technology, USA) force plates (1000 or 2400 Hz, respectively). Raw EMG signals from 8 major knee muscles were acquired from the skin-surface on the reconstructed (ACLRs) or randomized (controls) limb-side using Wave Wireless (CMR) (Zero Wire, Aurion, Italy) or Telemyo 900 (CHESM) (Noraxon, Arizona, USA) systems (1000 or

2400 Hz, respectively). Using our previously described procedures (12, 17, 51), which adhere to the SENIAM guidelines (<http://www.seniam.org/>), the skin-surface was prepared and then pre-formed bipolar Ag/AgCl electrodes (Duo-Trode, Myotronics, USA) were applied to the medial and lateral *gastrocnemii*, hamstrings and *vasti* as well as *rectus femoris* and *tensor fasciae latae*.

Marker trajectories, GRFs and EMGs were processed by custom Matlab (The Mathworks, USA) scripts. All data filtering used 4th order zero-lag Butterworth filters. Markers and GRFs were low-pass filtered with 10 and 15 Hz cut-off frequencies for walking and running/sidestepping, respectively. The raw EMGs were band-pass filtered (30-500 Hz pass-band), full-wave rectified and low-pass filtered (6 Hz cut-off frequency) to produce linear envelopes. While the two EMG acquisition systems operated at different sampling frequencies, because they both sampled above the Nyquist limit for skin-surface EMG from lower-limb muscles the final linear envelopes (filtered at 6 Hz) were not affected. Each EMG envelope was subsequently scaled to their maximum value identified from all trials recorded from the individual, *i.e.* specific maximum exertion isometric and isokinetic trials, as well as all of dynamic tasks.

The gait biomechanics of each participant were modelled using OpenSim (11) v3.2. A customized anatomic model, based on the generic running simulation model (18), was used. The customization included modifying the standard one degree of freedom (DOF) tibiofemoral joint (53) to permit 15°/5° internal/external rotations, while locking the adduction/abduction rotations. This enabled the determination of three net moments at the knee and prevented non-physiological knee motion. We chose to allow knee internal/external rotations and lock knee adduction/abduction rotations based on bone-pin derived knee kinematics (5) and *in vivo* instrumented prosthetic knee implant contact forces (15). First, when used to compute knee

kinematics, skin-surface markers have not accurately measured knee adduction/abduction rotations. During sidestepping, skin-surface methods measured the opposite knee adduction/abduction rotations compared to the gold standard of bone-pin measurement (see (5), Figure 4, subplot 2-2). In contrast, knee internal/external rotations were well characterized by skin-surface markers, showing similar shape to bone-pin measurements and have half of the adduction/abduction error (see (5), Table 2). Second, instrumented prosthetic knee implants (15) clearly show that the lateral femoral condyle and tibial plateau remain in contact throughout the gait cycle, and that no period of lateral compartment lift-off occurs. Therefore, the knee adduction/abduction rotations that have been reported (5) are due to the geometry of the tibiofemoral articulating surfaces. Indeed, it is possible to create a mechanism to describe the detailed passive motion of the knee (34), however, this was beyond the scope of this current study. Therefore, we used a knee model that prevented condylar lift-off as has been done in the past (Winby et al 2009, Gerus et al 2013), while allowing the knee internal-external rotations that can be measured with skin-surface markers.

Within the tibiofemoral mechanism, two contact points were positioned in the medial and lateral tibial compartments, respectively. They were positioned using a femoral condyle regression method (51) that estimated the location of the tibiofemoral contact points based on the width of skin-surface markers placed on the femoral condyles. These contact points were fixed in position and did not change with knee motion, but enabled the determination of net moments and muscle tendon unit actuator (MTUA) moments arms relative to the medial and lateral tibial compartments which were needed to solve our model of knee contact dynamics (51).

The customized anatomic model was then scaled, registered and optimized to each participant's dimensions, static posture and experimental marker configuration. Scaling used prominent

bony landmarks and joint centres to linearly adjust the model's dimensions, mass and inertia. Then a systematic registration method (13) was used to map each participant's experimental configuration (*i.e.* marker positions and static posture) to the model. The registration method involved calculating a set of anatomically based segment frames from experimental skin-surface markers acquired during a standing static trial. These anatomical frames were then used to compute direct kinematic joint angles and to determine the local position of marker clusters on each body segment. Joint angles and local marker cluster positions were then applied to the scaled anatomic model, and optimized to reduce fitting error. Importantly, this systematic registration method has been shown to improve the accuracy of subsequent model dynamics (13).

The muscle parameters within the anatomic model do not necessarily scale linearly with body dimensions (46). Therefore, after scaling and registration, we optimized the tendon slack and optimal fibre lengths for each MTUA to preserve their operating characteristics, as proposed by Winby et al (52) and robustly implemented more recently (30). To account for autograft donor muscle impairment in the ACLR participants, the *semitendinosus* was modified (*gracilis* was not included in the anatomic model since its EMG was not recorded). Williams et al (50) reported reductions of 19% in cross-sectional area (CSA) and 44% in volume of the donor *semitendinosus*, compared to the contralateral muscle, measured post-ACLR at the time of return to sports. Assuming that the *semitendinosus* pennation angle remained constant and that cross-section area (CSA) is a proxy of physiological CSA, the optimal fibre length of the *semitendinosus* of the ACLR participants in this study was modified

$$OptFL_{Semi}^{ACLR} = OptFL_{Semi}^{Contra} * \frac{V_{Semi}^{ACLR}}{V_{Semi}^{Contra}} * \frac{CSA_{Semi}^{Contra}}{CSA_{Semi}^{ACLR}},$$

and the *semitendinosus* maximum isometric strength modified

$$MaxIso_{Semi}^{ACLR} = MaxIso_{Semi}^{Contra} * \frac{CSA_{Semi}^{ACLR}}{CSA_{Semi}^{Contra}} ,$$

where, $OptFL_{Semi}^{ACLR}$ and $OptFL_{Semi}^{Contra}$ were ACLR and contralateral *semitendinosus* optimal fibre lengths, V_{Semi}^{ACLR} and V_{Semi}^{Contra} were ACLR and contralateral *semitendinosus* volumes, CSA_{Semi}^{ACLR} and CSA_{Semi}^{Contra} were ACLR and contralateral *semitendinosus* CSA, and $MaxIso_{Semi}^{ACLR}$ and $MaxIso_{Semi}^{Contra}$ were ACLR and contralateral *semitendinosus* maximum isometric strengths. In the above equations, the measurements of the contralateral *semitendinosus* were taken post-surgery at the time of return to sport, but were not significantly different from the pre-surgery volume and CSA measurements.

The ACLR *semitendinosus* optimal fibre length was reduced

$$OptFL_{Semi}^{ACLR} = OptFL_{Semi}^{Contra} * 0.69 ,$$

and maximum isometric strength reduced

$$MaxIso_{Semi}^{ACLR} = MaxIso_{Semi}^{Contra} * 0.81 ,$$

Williams et al (50) reported no significant change in ACLR *semitendinosus* tendon CSA, thus we assumed standard normalized tendon stiffness that scaled with the muscle's maximum isometric force. To ensure the adjusted ACLR *semitendinosus* MTUA operating range conformed to standard values, we optimized the tendon slack length such that the normalized tendon force-length relationship and the overall MTUA length were preserved throughout a set of multi-DOF lower-limb joint angles (30).

Joint kinematics and moments, as well as MTUA kinematics, for walking, running and sidestepping gait tasks were then determined for each participant using the OpenSim inverse kinematics, inverse dynamics and muscle analysis tools, respectively. Gait biomechanics,

MTUA kinematics and parameters, as well as processed EMGs, were then used to calibrate and drive an EMG-driven neuromusculoskeletal model of muscle force (25) with an embedded tibiofemoral contact model (51). For each participant, walking, running, and sidestepping trials were used to calibrate the EMG-driven neuromusculoskeletal model, which then determined muscle and tibiofemoral contact forces for the subsequent trials. After calculating the EMG-driven tibiofemoral contact forces, we performed a preliminary assessment of the model by comparing ACLR and control contact forces against instrumented knee implants (details in Appendix).

All biomechanical data were normalized to 100% of the gait cycle for walking and 100% of stance for running and sidestepping. Gait analysis outcomes included the spatiotemporal parameters (Table 1), external knee moments, knee angles, ranges of motion and the tibiofemoral contact forces, all calculated from the stance phase of the different gait tasks. The maximum eKAM and external knee flexion moment (eKFM) were calculated, as were the maximum knee flexion angle (KFA), angle at heel strike (KFAh), and excursion (KFE). Similarly, the maximum knee internal (KIA) and external (KEA) rotations, internal/external rotation angle at heel strike (KIEAh) and internal/external (KIEE) rotation excursion were calculated. The EMG-driven variables were maximum total tibiofemoral (TTF), MTF and LTF contact forces. The mean relative muscle and external load contributions to the MTF and LTF contact forces during stance were also determined as described by Winby and colleagues (51). In the frontal plane of the knee, the external moments, muscle and other soft tissue moments, and the moments generated due to contact forces equilibrate. Following Winby and colleagues' (51) notation, we calculated the relative (*i.e.* percentage) contribution made by all the muscles and the external loads (*i.e.* the external frontal plane moments about the relevant tibiofemoral compartment) to the contact loading experienced by the MTF and LTF compartments. For each participant, an average of three repeats of each gait task were analysed. Intra-trial correlations

for the knee flexion angles were calculated for walking (ACLR: $R^2=0.98\pm0.01$, controls: $R^2=0.99\pm0.02$), running (ACLR: $R^2=0.97\pm0.05$, controls: $R^2=0.98\pm0.01$), and sidestepping (ACLR: $R^2=0.98\pm0.02$, controls: $R^2=0.98\pm0.02$). The repeated trials were then averaged to produce a single curve for each measure for each participant. The above listed gait biomechanics and tibiofemoral contact force parameters were then calculated for each participant from their averaged curves. These parameters were then used for the statistical analysis between the ACLRs and controls.

All variables were statistically analysed using SPSS v22 (IBM, Armonk, NY) and significance was set to $p<0.05$. Group differences in participant characteristics were tested using Student's t-tests and Chi-squared. Main effects of, and interactions between, group and gait task on all outcome measures were tested using 2x3 mixed ANOVAs (group as the between measure and gait task as the repeated measure). If main effects were found, post-hoc t-tests with a Bonferroni correction for multiple comparisons were applied to assess specific paired differences.

Results

The ACLR and control EMG-driven walking tibiofemoral contact forces showed moderate-to-strong correlations with instrumented implant contact forces (Appendix).

No significant differences were found between the ACLR and control groups for sex, age, height, tested limb-side or discrete gait spatiotemporal parameters (Table 1). Although, the mean body mass of the ACLRs (78.1 ± 14.4 kg) was significantly greater than the controls (67.8 ± 14.0) ($p<0.0001$).

The maximum knee flexion-extension angle, angle at heel strike and excursion parameters (KFA, KFAh, KFE) were significantly different between groups (all $p<0.05$). During walking, the maximum KFA trended towards smaller ($p=0.1$) in the ACLRs ($17\pm6.4^\circ$) compared to

controls ($19\pm 5.0^\circ$). During running, the ACLR maximum KFA ($41.4\pm 6^\circ$) was significantly smaller compared to controls ($44\pm 5.9^\circ$) ($p=0.01$). Similarly, during sidestepping the ACLR KFA ($50.6\pm 6.9^\circ$) was significantly smaller compared to controls ($53.4\pm 7.3^\circ$) ($p=0.01$) (Figure 1, A). No significant group differences were found in the KFAh during walking (ACLR= $1.23\pm 4.1^\circ$, controls= $1.20\pm 4.2^\circ$), running (ACLR= $16.1\pm 5.7^\circ$, controls= $18.0\pm 6.3^\circ$) or sidestepping (ACLR= $19.2\pm 7.0^\circ$, controls= $18.6\pm 8.0^\circ$). During walking, the KFE was similar between ACLRs ($40.6\pm 4.7^\circ$) and controls ($41.2\pm 4.9^\circ$), but during running was significantly smaller in the ACLRs ($32.4\pm 5.4^\circ$) compared to controls ($35.4\pm 4.6^\circ$) ($p=0.01$), as well as during sidestepping (ACLR= $39.9\pm 6.7^\circ$, controls= $42.5\pm 7.1^\circ$) ($p=0.02$) (Figure 1, B). No main effects of groups, nor interactions of group with gait task, were found for any of the knee internal/external rotation parameters.

The eKFM was significantly different between groups (Figure 1, C) ($p=0.001$). During walking, the maximum eKFM in the ACLRs ($0.052 \text{ Nm}\cdot\text{kg}^{-1}$) trended towards smaller than the controls ($0.061 \text{ Nm}\cdot\text{kg}^{-1}$) ($p=0.1$). During running, maximum eKFM in ACLRs ($0.25\pm 0.08 \text{ Nm}\cdot\text{kg}^{-1}$) was significantly smaller compared to controls ($0.29\pm 0.06 \text{ Nm}\cdot\text{kg}^{-1}$) ($p=0.002$), and similarly during sidestepping (ACLR= $0.29\pm 0.1 \text{ Nm}\cdot\text{kg}^{-1}$, controls= $0.33\pm 0.1 \text{ Nm}\cdot\text{kg}^{-1}$) ($p=0.01$). No significant group differences were found for the maximum eKAM (Figure 1, D). No significant interactions between group and gait task were found for any of the gait analysis variables.

A significant main effect between ACLRs and controls was found for maximum TTF and MTF contact forces scaled to bodyweight ($p<0.0001$), but not for maximum LTF contact force ($p=0.08$). The maximum TTF contact forces in ACLRs were significantly smaller during walking ($2.38\pm 0.52 \text{ BW}$, $p<0.0001$), running ($6.98\pm 1.08 \text{ BW}$, $p=0.001$) and sidestepping ($7.22\pm 1.35 \text{ BW}$, $p<0.0001$) compared to controls: $2.83\pm 0.64 \text{ BW}$, $7.83\pm 1.48 \text{ BW}$ and

8.47±1.57 BW, respectively (Figure 2). Similarly, significantly smaller maximum MTF contact forces in ACLRs were found during walking (1.48±0.34 BW, $p=0.009$), running (4.49±0.77 BW, $p<0.0001$) and sidestepping (3.62±0.9 BW, $p<0.0001$), compared to controls: 1.82±0.47 BW, 5.1±0.95 BW and 4.62±0.83 BW, respectively (Figure 2). A subgroup analysis of the ACLR individuals who sustained isolated ACLR and those with ACLR and meniscal injury was performed, and no significant differences between the subgroups were found for the maximum tibiofemoral contact forces. A significant main effect of gait task was found for the ACLR and control groups ($p<0.0001$). The maximum TTF and LTF contact forces (Figure 2) significantly increased (~3-4 times) from walking, to running to sidestepping, while maximum MTF contact force peaked during running for both groups (all $p<0.0001$). No significant interactions between group and gait task for the tibiofemoral contact forces were found in this study. When the tibiofemoral contact forces were not scaled to bodyweight, the maximum raw contact forces were not significantly different between ACLRs and controls (Table 2).

No significant main effects of group, or interactions between group and gait task, were found for the mean relative muscle and external load contributions to the tibiofemoral contact forces (Figures 3 and 4). However, a significant main effect of gait task was found ($p<0.0001$) where the mean relative muscle contributions to the MTF (Figure 3) and LTF (Figure 4) contact forces increased significantly from walking (~50% and 65%) to running (85% and 90%) (all $p<0.0001$). During sidestepping the mean relative muscle contributions to MTF contact force remained ~90%, and decreased to 80% for the LTF compartment ($p<0.0001$).

Discussion

The purpose of this study was to use an EMG-driven neuromusculoskeletal model to investigate the possible differences between ACLR individuals and healthy controls in terms of the contact forces experienced within the tibiofemoral joint during different gait tasks. First,

we performed a limited validation of the EMG-driven model and found the model predicted contact forces of similar magnitude, shape, distribution and timing as instrumented prosthetic knee implant data (Appendix). Second, we examined the tibiofemoral contact forces, and the contributions to those contact forces made by muscle and external loads, in the ACLRs and controls during the different gait tasks. When scaled to bodyweight, we found smaller magnitude maximum TTF and MTF contact forces in the ACLRs compared to controls across the different gait tasks. Similarly, compared to the controls, we found a smaller maximum eKFM, maximum KFA, and KFE in the ACLRs during running and sidestepping, and a trend towards smaller during walking. The relative muscle and external load contributions were not significantly different between the ACLRs and controls, nor were either the maximum eKAM or the knee internal/external rotation parameters. This is, to our knowledge, the first study to examine the tibiofemoral contact forces in these gait tasks for an ACLR population in comparison with healthy controls.

Contrary to our first hypothesis, the maximum TTF and MTF contact forces (scaled to BW) in the ACLR individuals were smaller than the controls during the different gait tasks, a mechanical condition we refer to as “lower-loading” for the remainder of this discussion. We had anticipated that ACLR individuals would have larger MTF contact forces compared to the controls during walking, based on literature reports of a larger walking eKAM in ACLRs (9). Furthermore, compared to healthy controls, ACLRs have been shown to have larger TTF contact forces during drop-landing (42). Therefore, we had expected larger tibiofemoral contact forces in ACLRs during other similarly demanding motor tasks such as running and sidestepping. More generally, we expected larger tibiofemoral contact forces in the ACLRs because it has been well established that 1) ACLR individuals are at risk of knee OA development (3), and 2) increased MTF contact loading (*i.e.* inferred by surrogate measures) has been shown to be related to both incident MTF articular cartilage damage (37) and OA

progression (4, 29). Thus, we had a basis to expect the ACLR knee to have larger loading than a control knee. However, profound joint under-loading has also been shown to drive joint degeneration, whether due to Botox-induced muscle weakness (14) or following spinal cord injury (43). Importantly, in comparison to the contralateral knee, the ACLR knee has been shown to have reduced MTF contact forces during walking gait, and this lower-loading was associated with the early onset of medial knee OA (49). During walking, the differences between the ACLRs and controls in the bodyweight-scaled tibiofemoral contact forces (~10-15% lower in ACLRs) were similar to the previously reported asymmetry values in ACLRs (16). A deficit of ~14% BW in the ACLR knee compared to the contralateral knee was reported (16), but follow-up testing (49) showed that by 1-5 years post-ACLR the knee contact loads during walking were symmetrical. In contrast, the ACLRs in this study were tested at a mean time from surgery of 2.51 ± 0.44 years and yet we still found differences in the bodyweight-scaled tibiofemoral contact forces. This may be due to the highly variable path to full recovery following ACLR (19), and our sample population of ACLR individuals that was composed of both those who had and had not returned to sport participation.

Similar to walking, the tibiofemoral contact forces (scaled to BW) during running and sidestepping were found to be smaller in the ACLRs compared to the controls. The magnitudes were found to be comparable in these gait tasks to those predicted during drop-landing (42). Importantly, the drop-landing study (42) was the only previous study to have investigated differences in tibiofemoral contact forces between ACLRs and healthy controls, and similarly sought to scale their estimates of the tibiofemoral contact forces to participant body mass. Our findings of total tibiofemoral contact forces during running and sidestepping in the ACLR individuals $>100 \text{ N}\cdot\text{kg}^{-1}$ and reduced knee flexion were consistent with the report by Tsai and colleagues (42). Unfortunately, Tsai and colleagues (42) did not report the external knee moments from their tests, thus limiting this aspect of comparison between the studies. They

found their ACLR group had larger total mass-scaled tibiofemoral contact forces than the controls, while we found the opposite. Importantly, they examined a small sample of ACLRs with mixed autograft-types (n=10) and healthy controls (n=10). It may be that their findings were specific to the performance of drop-landing by ACLRs and/or a peculiar feature of the all-female sample they examined.

In our study, and in the previous investigations (20, 26, 42, 49), each participant's tibiofemoral contact forces were scaled to their body mass (45) or weight (21, 26, 53). The rationale for scaling is that heavier individuals will have larger tibiofemoral contact forces, and thus to compare different populations some form of normalization of the magnitudes of the contact forces is required. However, the articular tissues respond to the actual loading applied to the contact area within the tissue, not to loading normalized to body mass or weight. In this study, we found that, despite the ACLRs being significantly heavier than the controls, the raw tibiofemoral contact forces were not significantly different between ACLRs and controls. Moreover, these same ACLRs and half of the control group have previously been shown (45) to have tibial bone plate areas (*i.e.* the size of the knee) that were similar, but the ACLRs had less tibial articular cartilage volume with more defects. This means that at the level of the articular cartilages in both the ACLRs and controls, similar articular contact forces were applied to knees of similar size, however, the structure of the tibiofemoral articular cartilage in the ACLRs was poorly suited to sustaining these loads (*i.e.* smaller tissue with more holes in it). Thus, under the substantial tibiofemoral contact loading present during tasks such as running and sidestepping the tibiofemoral articular cartilages in these ACLR individuals may be at risk of structural damage.

None of the gait spatiotemporal parameters (*i.e.* speeds, stride lengths and cadences), maximum GRF (scaled to bodyweight), or maximum eKAM were statistically different between the

groups. The ACLR group was statistically heavier than the controls, which, if all else were equal, would have increased the magnitude of the tibiofemoral contact forces, but this was not observed. Importantly, compared to the controls, the maximum eKFM in the ACLRs was smaller during both running and sidestepping, and trended towards smaller during walking ($p=0.1$). The eKFM during gait is balanced primarily by the action of the knee muscle flexor and extensor moments (*i.e.* the quadriceps, hamstrings and *gastrocnemii*). As these muscles have substantial *varus* and *valgus* moment arms (7), their activation has considerable effect on the magnitude of the tibiofemoral contact forces. The importance of the eKFM to the magnitude of the tibiofemoral contact forces has been highlighted in recent neuromusculoskeletal modelling (26) and instrumented knee implant (28) studies. Thus, the smaller maximum eKFM moment in the ACLR individuals compared to controls during running and sidestepping explained the smaller maximum TTF and MTF contact forces (scaled to BW), and also explained the similar magnitude raw tibiofemoral contact forces despite the substantially heavier ACLR group.

In addition to the eKFM, a smaller maximum KFA and KFE were found in the ACLRs compared to controls. A smaller KFE means that the total area of contact between the tibiofemoral articulating surfaces in each gait cycle would be reduced. Thus, while the magnitudes of the raw tibiofemoral contact forces were similar between the ACLRs and controls, those articular contact forces were focused to smaller regions within the ACLR tibiofemoral joint. This is relevant because femoral articular cartilage thickness distribution has been shown to be related to knee flexion during walking in both healthy individuals (22) and ACLR patients (36). Moreover, the loss of knee extension, reported in this study (Figure 1) as well as in meta-analysis of the literature (39), has been shown to be related to poor long-term knee health following ACLR (38). However, without a long-term follow-up on these ACLR

individuals we cannot comment on any potential effects of knee kinematics on future knee health.

Knee internal/external rotation has the potential to alter regional articular contact loading patterns. Andriacchi and colleagues (1) have proposed an explanatory framework of joint degeneration following ACL injury, and, while it has been applied primarily to ACL deficient knees, the relevance to ACLR has been acknowledged (10). Under this framework, a rotational shift of the tibia transfers the large tibiofemoral articular contact forces produced during daily activity to regions unaccustomed to these loads. As the capacity of adult articular cartilage to adapt is limited (27), such abrupt changes in regional articular cartilage contact loading potentially place the unaccustomed regions at risk for degeneration. However, in the current investigation we did not find any significant differences between the ACLRs and controls in the tested knee internal/external rotation parameters. Moreover, there have been equivocal reports regarding the effect of ACLR on knee internal/external rotation (32, 35, 54). The lack of consensus on the effect of ACLR on knee internal/external rotations under dynamic loading conditions may partly be explained by the different experimental designs (*i.e.* cadaver *vs.* living humans and walking *vs.* other motor tasks), surgical techniques (*i.e.* autograft type and alignment), and biomechanical methods and models. Importantly, the reported external rotation offset of the tibia in cadaver ACLR knees (54) was within the range of error associated with skin-surface marker based measurements of knee internal/external rotations (5). Thus, to non-invasively measure such small differences *in vivo* may require robust methods to reduce soft tissue artefact or dynamic radiographic imaging.

The eKAM has the potential to alter the magnitude of the tibiofemoral contact forces and change the distribution of loading between the medial and lateral tibiofemoral compartments. However, the eKAM was not found to be statistically different between the ACLRs and

controls, suggesting an equivalence between the groups in terms of the tibiofemoral compartmental load distributions that was confirmed by our model predictions. Studies of the effect of ACLR on the eKAM during walking have produced conflicting results, with smaller (47), larger (9) and equivalent (48) magnitudes reported. However, these previous studies had modest sample sizes (16-48 ACLR participants), tested individuals who had received different autograft-types (hamstrings and bone patellar tendon bone), and performed gait at different time points following ACLR, making it difficult to draw definitive conclusions from the results. The current study used a large sample (n=104) of both males and females, with a homogeneous autograft-type, tested at a similar time point following ACLR (2.51 ± 0.44 years) compared to a large sample of healthy controls (n=60). Furthermore, these ACLR individuals had spatiotemporal parameters (walking speed, cadence and GRFs) statistically equivalent to the control group for all tested gait tasks. This is important because if one walks faster the joint contact loads increase (24), but this was not observed. Rather, our results were consistent with those of Webster and colleagues (48), and indicated that the maximum eKAM in the ACLRs was similar to that of healthy controls during the different gait tasks.

Differences in the relative contribution of muscle and external loads could also have affected the magnitude and distribution of the tibiofemoral contact forces, but this did not occur, disagreeing with our second hypothesis. We had hypothesized that the relative contributions of muscle to MTF contact forces would be decreased in the ACLRs compared to controls, due to a previously reported larger eKAM during walking (9), but, as noted above, we found the maximum eKAM to be equivalent between the two groups. However, the eKAM is only a net measure of knee frontal plane loading, and does not directly account for the load sharing between the many internal knee structures, including the muscles (51). Therefore, even with an equivalent eKAM between ACLRs and controls, it was possible that differences in muscle activation patterns would have changed the tibiofemoral load distribution. Indeed, it has been

demonstrated experimentally that modulating the magnitude of the eKAM through targeted gait intervention did not necessarily produce concomitant changes in the MTF contact force (44). Importantly, the mean relative contributions of muscle to the tibiofemoral contact forces were not statistically different between the ACLR individuals and healthy controls. This meant that the differences in the magnitude of the maximum tibiofemoral contact forces (scaled to BW) between the groups were explained by the action of muscles generating different eKFM (as discussed above), and not by changing the relative role of muscles stabilizing the eKAM.

There were limitations to this current study. First, muscle activation patterns are known to be abnormal in ACLR individuals (6, 42), and it is possible that our measures of the muscle activations in the ACLR individuals were not completely accurate. An ACLR individual may have not fully recruit their knee muscle fibres (6) resulting in a lower maximum EMG signal. When this “maximum” was then used in subsequent scaling of other EMGs for analysis this may have resulted in an overestimation of the level of activation. However, the effect of overestimating muscle activations in the ACLRs would likely have been to increase the tibiofemoral contact forces, thereby conservatively reducing differences when compared to the control values.

Second, our EMG-driven model presented the same limitations inherent to neuromusculoskeletal models applied to human movement: there exists no method to directly validate muscle force predictions and only limited data to validate the model estimates of the tibiofemoral contact force (17). However, EMG-driven models have been shown to well-predict the tibiofemoral contact forces measured using instrumented knee prostheses (17, 51).

Third, the model we used to estimate the tibiofemoral contact forces was sensitive to contact geometry (23). We did not have a truly subject-specific contact model, but used a personalized method to position the contact points (51). However, it should be noted, that even with a

subject-specific contact geometry, the contact model we used assumed that the contact points do not change position on the tibia with knee motion and thus should be considered a limitation of this method.

Fourth, we chose to adjust the model of the ACLR semitendinosus to reflect the impairment to this autograft donor muscles using measurements reported in the literature (50). The literature measurements were taken from ACLR individuals at 6 months post-operation, while in our study the ACLRs were tested at 2-3 years post-operation. If our sample of ACLRs had substantially different levels of regeneration of their harvested tendons compared to those previously reported, this would make our adjustments inaccurate. However, a recent study (21) has shown that substantial atrophy in the autograft donor *semitendinosus* is present at ~2.5 years following a similar ipsilateral *semitendinosus* and *gracilis* tendon autograft ACLR. Nonetheless, our adjustments to the model of the *semitendinosus*, while personalized through morphometric scaling (31), were not truly subject-specific (*i.e.* customized to each participant based on medical imaging of the lower-limb muscle anatomy). Thus, we cannot rule out that individual participants in our study had different levels of autograft donor site regeneration following ACLR than what we implemented within our model. We performed a simple investigation into the potential effects of harvesting the *semitendinosus* on the tibiofemoral contact forces to determine if it was worth the time and effort for researchers to account for donor site impairment in future research into ACLR knee biomechanics. To do this we modified the *semitendinosus* in the generic anatomic model to reflect the impairment following ACLR as described in our methods section. We then maximally activated the muscle through a nominal range of knee flexion angles (-10-120°) and compared the resulting tibiofemoral contact forces against values from an unmodified model (Appendix Figure 3). We found that the modified *semitendinosus* yielded mean reduction in the MTF contact forces of 28±7% across the range of knee flexion angles. This suggests that accounting for autograft donor site

impairment following ACLR has the potential to substantially alter the tibiofemoral contact forces. However, it should be acknowledged that reduced muscle strength and changed internal muscle parameters may not have intuitive or simple effects on the tibiofemoral contact forces. Human muscle systems, and the computational frameworks used to model them, are highly non-linear and dynamic. Thus, modifications to one muscle's strength and morphology may cause compensations in movement, muscle activation patterns, and, over time, potentially the morphology of surrounding muscles. To fully explore the effects of ACLR donor muscle impairment was beyond the scope of this study, but we are currently pursuing a more comprehensive investigation.

Finally, the ACLR group included individuals who had sustained an isolated ACL rupture as well as those who had sustained ACL with meniscal injury. A subgroup analysis did not reveal any statistical differences in the tibiofemoral contact forces or gait biomechanics, but future studies properly powered should consider exploring potential differences between these subgroups.

In conclusion, the ACLR individuals had smaller maximum TTF and MTF contact forces (scaled to bodyweight) compared to the healthy controls for all tested gait tasks and similar magnitude raw tibiofemoral contact forces. The ACLR individuals also had smaller maximum eKFM, KFA and KFE during running and sidestepping, and displayed a trend towards smaller values during walking. The maximum eKAM was similar between ACLRs and controls. The relative contributions made by muscle and external loads to the MTF and LTF contact forces were not significantly different between ACLRs and controls, although they increased for both groups from walking, to running, and sidestepping (up 80-90% of contact forces).

Conflict of Interest Statement

No conflicts.

Acknowledgements

The results of the present study do not constitute endorsement by ACSM. We acknowledge funding support for this research from the Australian National Health and Medical Research Council (to ALB, DGL, KLB and FMC) (grant # 628850) and National Health and Research Council R.D Wright Biomedical Fellowship (to ALB) and Principal Research Fellowship (to KLB). David Saxby would like to acknowledge Griffith University for PhD scholarship and stipend awards as well as the International Society of Biomechanics for a PhD Matching Dissertation Grant. The authors would like to acknowledge Prof BJ Fregly of the University of Florida for contribution of Grand Challenge instrumented knee implant data (<https://simtk.org/home/kneeloads>), as well as Dr.'s Alasdair Dempsey and Nicole Grigg for their contributions to data collection.

References

1. Andriacchi TP, Mundermann A, Smith RL, Alexander EJ, Dyrby CO, Koo S. A framework for the in vivo pathomechanics of osteoarthritis at the knee. *Annals of Biomedical Engineering*. 2004;32(3):447-57.
2. Armour T, Forwell L, Litchfield R, Kirkley A, Amendola N, Fowler PJ. Isokinetic evaluation of internal/external tibial rotation strength after the use of hamstring tendons for anterior cruciate ligament reconstruction. *American Journal of Sports Medicine*. 2004;32(7):1639-43.
3. Barenius B, Ponzer S, Shalabi A, Bujak R, Norlen L, Eriksson K. Increased risk of osteoarthritis after anterior cruciate ligament reconstruction: a 14-year follow-up study of a randomized controlled trial. *American Journal of Sports Medicine*. 2014;42(5):1049-57.
4. Bennell KL, Bowles KA, Wang Y, Cicuttini F, Davies-Tuck M, Hinman RS. Higher dynamic medial knee load predicts greater cartilage loss over 12 months in medial knee osteoarthritis. *Annals of the Rheumatic Diseases*. 2011;70(10):1770-4.
5. Benoit DL, Ramsey DK, Lamontagne M, Xu L, Wretenberg P, Renstrom P. Effect of skin movement artifact on knee kinematics during gait and cutting motions measured in vivo. *Gait & Posture*. 2006;24(2):152-64.
6. Bryant AL, Kelly J, Hohmann E. Neuromuscular adaptations and correlates of knee functionality following ACL reconstruction. *Journal of Orthopaedic Research*. 2008;26(1):126-35.
7. Buchanan TS, Kim AW, Lloyd DG. Selective muscle activation following rapid varus/valgus perturbations at the knee. *Medicine & Science in Sports & Exercise*. 1996;28(7):870-6.

8. Burks RT, Crim J, Fink BP, Boylan DN, Greis PE. The effects of semitendinosus and gracilis harvest in anterior cruciate ligament reconstruction. *Arthroscopy*. 2005;21(10):1177-85.
9. Butler RJ, Minick KI, Ferber R, Underwood F. Gait mechanics after ACL reconstruction: implications for the early onset of knee osteoarthritis. *British Journal of Sports Medicine*. 2009;43(5):366-70.
10. Chaudhari AM, Briant PL, Bevill SL, Koo S, Andriacchi TP. Knee kinematics, cartilage morphology, and osteoarthritis after ACL injury. *Medicine & Science in Sports & Exercise*. 2008;40(2):215-22.
11. Delp SL, Anderson FC, Arnold AS et al. OpenSim: open-source software to create and analyze dynamic simulations of movement. *IEEE Transactions on Bio-medical Engineering*. 2007;54(11):1940-50.
12. Dempsey AR, Lloyd DG, Elliott BC, Steele JR, Munro BJ, Russo KA. The effect of technique change on knee loads during sidestep cutting. *Medicine & Science in Sports & Exercise*. 2007;39(10):1765-73.
13. Dunne J, Besier TF, Lloyd DG, Lay B, Delp SL, Seth A. Automated marker registration improves OpenSim joint angle and moment estimates of a humanoid robot (Abstract). In: *Proceedings of the International Society of Biomechanics Congress XXIV, 2013*. 2013: Natal, Brasil.
14. Egloff C, Sawatsky A, Leonard T, Hart DA, Valderrabano V, Herzog W. Effect of muscle weakness and joint inflammation on the onset and progression of osteoarthritis in the rabbit knee. *Osteoarthritis and Cartilage*. 2014;22(11):1886-93.
15. Fregly BJ, Besier TF, Lloyd DG et al. Grand challenge competition to predict in vivo knee loads. *Journal of Orthopaedic Research*. 2012;30(4):503-13.

16. Gardinier ES, Di Stasi S, Manal K, Buchanan TS, Snyder-Mackler L. Knee contact force asymmetries in patients who failed return-to-sport readiness criteria 6 months after anterior cruciate ligament reconstruction. *American Journal of Sports Medicine*. 2014;42(12):2917-25.
17. Gerus P, Sartori M, Besier TF et al. Subject-specific knee joint geometry improves predictions of medial tibiofemoral contact forces. *Journal of Biomechanics*. 2013;46(16):2778-86.
18. Hamner SR, Seth A, Delp SL. Muscle contributions to propulsion and support during running. *Journal of Biomechanics*. 2010;43(14):2709-16.
19. Hartigan EH, Axe MJ, Snyder-Mackler L. Time line for noncopers to pass return-to-sports criteria after anterior cruciate ligament reconstruction. *Journal of Orthopaedics and Sports Physical Therapy*. 2010;40(3):141-54.
20. Khandha A, Manal K, Wellsandt E, Buchanan TS, Snyder-Mackler L. The onset of knee osteoarthritis after anterior cruciate ligament surgery is associated with early unloading followed by an extended period of normal loading. *Osteoarthritis and Cartilage*. 2015;23(Supplement 2):A101-A2.
21. Konrath J, Vertullo C, Kennedy B, Bush H, Barrett RS, Lloyd DG. The morphology and strength of hamstrings remain altered at 2 years following a hamstring graft in anterior cruciate ligament reconstruction. *American Journal of Sports Medicine*. Accepted.
22. Koo S, Rylander JH, Andriacchi TP. Knee joint kinematics during walking influences the spatial cartilage thickness distribution in the knee. *Journal of Biomechanics*. 2011;44(7):1405-9.

23. Lerner ZF, DeMers MS, Delp SL, Browning RC. How tibiofemoral alignment and contact locations affect predictions of medial and lateral tibiofemoral contact forces. *Journal of Biomechanics*. 2015;48(4):644-50.
24. Lerner ZF, Haight DJ, DeMers MS, Board WJ, Browning RC. The effects of walking speed on tibiofemoral loading estimated via musculoskeletal modeling. *Journal of Applied Biomechanics*. 2014;30(2):197-205.
25. Lloyd DG, Besier TF. An EMG-driven musculoskeletal model to estimate muscle forces and knee joint moments in vivo. *Journal of Biomechanics*. 2003;36(6):765-76.
26. Manal K, Gardinier E, Buchanan TS, Snyder-Mackler L. A more informed evaluation of medial compartment loading: the combined use of the knee adduction and flexor moments. *Osteoarthritis and Cartilage*. 2015;23(7):1107-11.
27. Mankin HJ. The response of articular cartilage to mechanical injury. *Journal of Bone & Joint Surgery - American Volume*. 1982;64(3):460-6.
28. Meyer AJ, D'Lima DD, Besier TF, Lloyd DG, Colwell CW, Jr., Fregly BJ. Are external knee load and EMG measures accurate indicators of internal knee contact forces during gait? *Journal of Orthopaedic Research*. 2013;31(6):921-9.
29. Miyazaki T, Wada M, Kawahara H, Sato M, Baba H, Shimada S. Dynamic load at baseline can predict radiographic disease progression in medial compartment knee osteoarthritis. *Annals of the Rheumatic Diseases*. 2002;61(7):617-22.
30. Modenese L, Ceseracciu E, Reggiani M, Lloyd DG. Estimation of musculotendon parameters for scaled and subject specific musculoskeletal models using an optimization technique. *Journal of Biomechanics*. 2015.
31. Modenese L, Ceseracciu E, Reggiani M, Lloyd DG. Estimation of musculotendon parameters for scaled and subject specific musculoskeletal models using an optimization technique. *Journal of Biomechanics*. 2016;49(2):141-8.

32. Papannagari R, Gill TJ, Defrate LE, Moses JM, Petruska AJ, Li G. In vivo kinematics of the knee after anterior cruciate ligament reconstruction: a clinical and functional evaluation. *American Journal of Sports Medicine*. 2006;34(12):2006-12.
33. Paul JP. Bioengineering studies of the forces transmitted by joints. II. Engineering analysis. In: RM Kenedi editor. *Biomechanics and related bioengineering topics*. London, UK.: Pergamon Press; 1965, pp. 369-80.
34. Sancisi N, Parenti-Castelli V. A new kinematic model of the passive motion of the knee inclusive of the patella. *Journal of Mechanisms and Robotics*. 2011;3(4):041003.
35. Scanlan SF, Chaudhari AM, Dyrby CO, Andriacchi TP. Differences in tibial rotation during walking in ACL reconstructed and healthy contralateral knees. *Journal of Biomechanics*. 2010;43(9):1817-22.
36. Scanlan SF, Favre J, Andriacchi TP. The relationship between peak knee extension at heel-strike of walking and the location of thickest femoral cartilage in ACL reconstructed and healthy contralateral knees. *Journal of Biomechanics*. 2013;46(5):849-54.
37. Sharma L, Chmiel JS, Almagor O et al. The role of varus and valgus alignment in the initial development of knee cartilage damage by MRI: the MOST study. *Annals of the Rheumatic Diseases*. 2013;72(2):235-40.
38. Shelbourne KD, Gray T. Minimum 10-year results after anterior cruciate ligament reconstruction: how the loss of normal knee motion compounds other factors related to the development of osteoarthritis after surgery. *American Journal of Sports Medicine*. 2009;37(3):471-80.
39. Shi DL, Wang YB, Ai ZS. Effect of anterior cruciate ligament reconstruction on biomechanical features of knee in level walking: a meta-analysis. *Chinese Medical Journal (English)*. 2010;123(21):3137-42.

40. Snow BJ, Wilcox JJ, Burks RT, Greis PE. Evaluation of Muscle Size and Fatty Infiltration with MRI Nine to Eleven Years Following Hamstring Harvest for ACL Reconstruction. *Journal of Bone & Joint Surgery - American Volume*. 2012;94-A(14):1274-82.
41. Thomas RH, Resnick D, Alazraki NP, Daniel D, Greenfield R. Compartmental evaluation of osteoarthritis of the knee. A comparative study of available diagnostic modalities. *Radiology*. 1975;116(3):585-94.
42. Tsai LC, McLean S, Colletti PM, Powers CM. Greater muscle co-contraction results in increased tibiofemoral compressive forces in females who have undergone anterior cruciate ligament reconstruction. *Journal of Orthopaedic Research*. 2012;30(12):2007-14.
43. Vanwanseele B, Eckstein F, Knecht H, Stussi E, Spaepen A. Knee cartilage of spinal cord-injured patients displays progressive thinning in the absence of normal joint loading and movement. *Arthritis & Rheumatism*. 2002;46(8):2073-8.
44. Walter JP, D'Lima DD, Colwell CW, Jr., Fregly BJ. Decreased knee adduction moment does not guarantee decreased medial contact force during gait. *Journal of Orthopaedic Research*. 2010;28(10):1348-54.
45. Wang X, Wang Y, Bennell KL et al. Cartilage morphology at 2-3 years following anterior cruciate ligament reconstruction with or without concomitant meniscal pathology. *Knee Surgery, Sports Traumatology, Arthroscopy*. 2015.
46. Ward SR, Smallwood LH, Lieber RL. Scaling of human lower extremity muscle architecture to skeletal dimensions (Abstract). In: *Proceedings of the ISB XXth Congress*. 2005: Cleveland, Ohio. p. 502.

47. Webster KE, Feller JA. The knee adduction moment in hamstring and patellar tendon anterior cruciate ligament reconstructed knees. *Knee Surgery, Sports Traumatology, Arthroscopy*. 2012;20(11):2214-9.
48. Webster KE, McClelland JA, Palazzolo SE, Santamaria LJ, Feller JA. Gender differences in the knee adduction moment after anterior cruciate ligament reconstruction surgery. *British Journal of Sports Medicine*. 2012;46(5):355-9.
49. Wellsandt E, Gardinier ES, Manal K, Axe MJ, Buchanan TS, Snyder-Mackler L. Decreased Knee Joint Loading Associated With Early Knee Osteoarthritis After Anterior Cruciate Ligament Injury. *American Journal of Sports Medicine*. 2016;44(1):143-51.
50. Williams GN, Snyder-Mackler L, Barrance PJ, Axe MJ, Buchanan TS. Muscle and tendon morphology after reconstruction of the anterior cruciate ligament with autologous semitendinosus-gracilis graft. *Journal of Bone & Joint Surgery - American Volume*. 2004;86-A(9):1936-46.
51. Winby CR, Lloyd DG, Besier TF, Kirk TB. Muscle and external load contribution to knee joint contact loads during normal gait. *Journal of Biomechanics*. 2009;42(14):2294-300.
52. Winby CR, Lloyd DG, Kirk TB. Evaluation of different analytical methods for subject-specific scaling of musculotendon parameters. *Journal of Biomechanics*. 2008;41(8):1682-8.
53. Yamaguchi GT, Zajac FE. A planar model of the knee joint to characterize the knee extensor mechanism. *Journal of Biomechanics*. 1989;22(1):1-10.
54. Yoo JD, Papannagari R, Park SE, DeFrate LE, Gill TJ, Li G. The effect of anterior cruciate ligament reconstruction on knee joint kinematics under simulated muscle loads. *American Journal of Sports Medicine*. 2005;33(2):240-6.

Figure 1. The maximum knee flexion angle (A) (degrees), excursion (B) (degrees) and moment (C) ($\text{Nm}\cdot\text{kg}^{-1}$), as well as the maximum knee adduction moment (D) ($\text{Nm}\cdot\text{kg}^{-1}$) \pm standard deviation in the ACLRs (white) and control (black). Walking, running and sidestepping values are represented in the first, second and third column, respectively. *denotes statistical significance <0.05 .

Figure 2. The mean tibiofemoral contact forces for the ACLR and controls, as well as the mean knee flexion angle, \pm standard deviation during the different gait tasks. The ACLRs are red, and the controls are in blue. Rows A, B, and C hold the medial, lateral and total tibiofemoral contact forces (in bodyweights), while row D hold the knee flexion angle (in degrees).

Figure 3. The mean of the ACLR (white) and control (black) net percentage contributions of muscle and external loads to the medial tibiofemoral contact forces \pm standard deviation during walking (A), running (B) and sidestepping (C) gait tasks.

Figure 4. The mean of the ACLR (white) and control (black) net percentage contributions of muscle and external loads to the lateral tibiofemoral contact forces \pm standard deviation during walking (A), running (B) and sidestepping (C) gait tasks.

Table 1. The mean \pm standard deviations of selected spatiotemporal parameters for the different gait tasks for the ACLRs and controls, as well participant descriptive statistics are presented.

Group	Gait Task	Speed (m·s ⁻¹)	Stride Length (m)	Stride Time (s)	Stride Rate (Hz)	Step Rate (Hz)	Stride Cadence (strides·min ⁻¹)	Step Cadence (steps·min ⁻¹)
Control	Walking	1.44±0.22	1.51±0.12	1.08±0.09	0.93±0.074	1.85±0.15	55.7±4.45	111±8.89
	Running	4.38±0.42 ^{**}	NA	NA	NA	NA	NA	NA
	Sidestepping	3.58±0.50 ^{**†}						
ACLR	Walking	1.41±0.18	1.51±0.10	1.11±0.06	0.91±0.05	1.81±0.10	54.4±2.89	109±5.79
	Running	4.51±0.48 ^{**}	NA	NA	NA	NA	NA	NA
	Sidestepping	3.70±0.65 ^{**†}						
	Participant #	Sex (Female: Male)	Age (years±std)	Mass (kg±std)	Body Mass Index (kg·m ⁻² ±std)	Height (m±std)	Tested Lower- Limb (Right: Left)	Time from Surgery to Testing (years)
Control	60	25:35	27.5±5.4	67.8±14.0	22.7±3.0	1.75±1.1	28:32	NA
ACLR	104	38:66	29.7±6.5	78.1±14.4 [*]	25.2±3.6 [*]	1.76±0.8	54:50	2.51±0.44

^{*}Significantly different from the control group, $p < 0.05$

^{**}Significantly different from walking

[†]Significantly different from running

Table 2. Raw tibiofemoral contact forces for the ACLRs and controls during walking, running and sidestepping gait tasks.

	Walking			Running			Sidestepping		
	TTF (N)	MTF (N)	LTF (N)	TTF (N)	MTF (N)	LTF (N)	TTF (N)	MTF (N)	LTF (N)
Control	1903±714	1187±514	835±376	5658±1449*	3653±970*	2153±700*	5860±1970	3096±1173 [†]	3022±957 [†]
ACLR	1900±550	1190±390	803±271	5248±1306*	3374±883*	2023±552*	5928±1780 [†]	2972±918 [†]	3157±1252 [†]

*Significantly different from walking

[†]Significantly different from running

Figure 1. Rigid body external knee biomechanics

[Click here to download Figure 4x3_aclrCtrl_rigidKneeMechanics.tif](#)

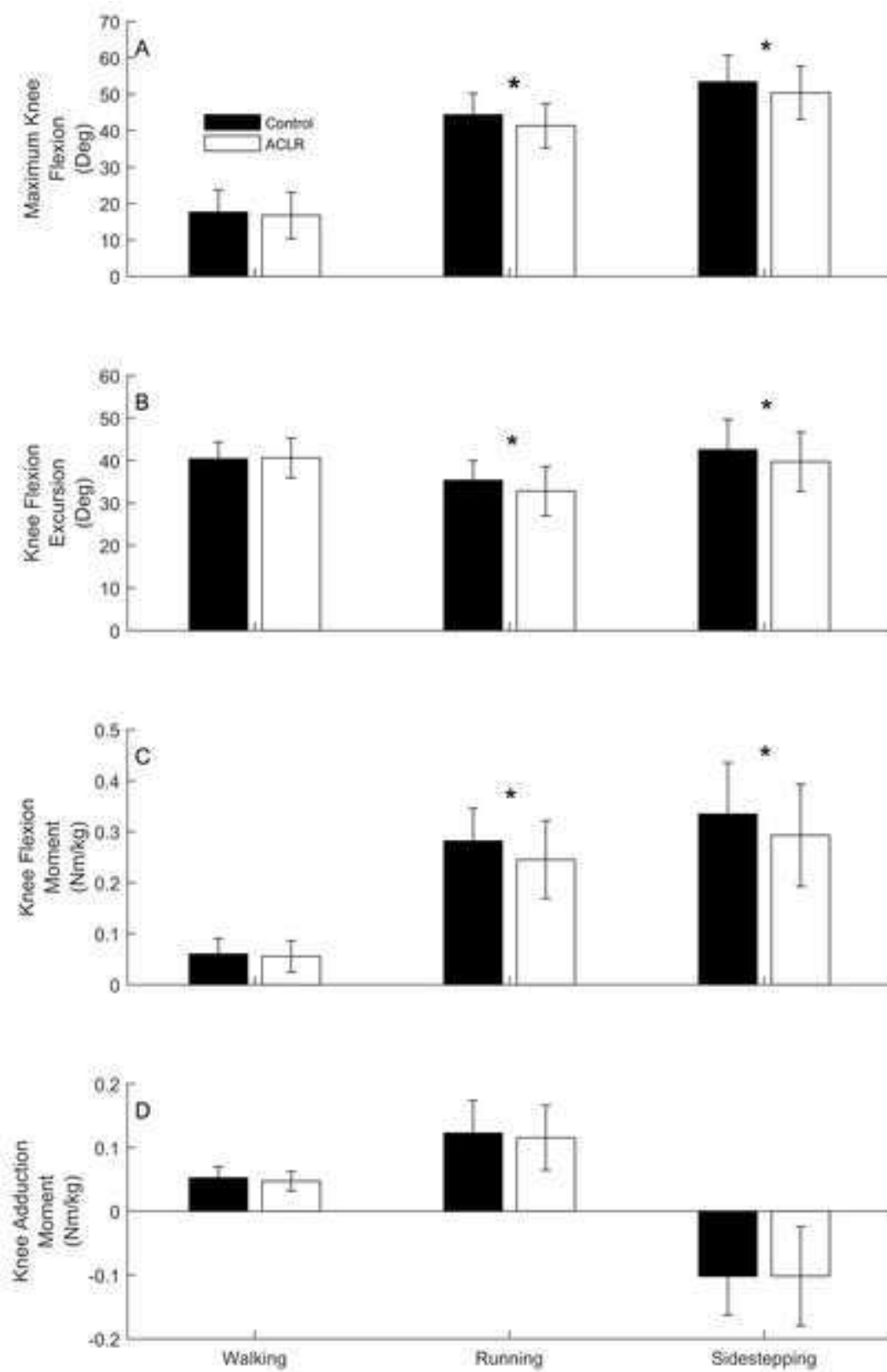


Figure 2. Tibiofemoral contact forces and knee flexion angles during all gait tasks

[Click here to download Figure 4x3_aclrCtrl_ContactForcesAndKFA.tif](#)

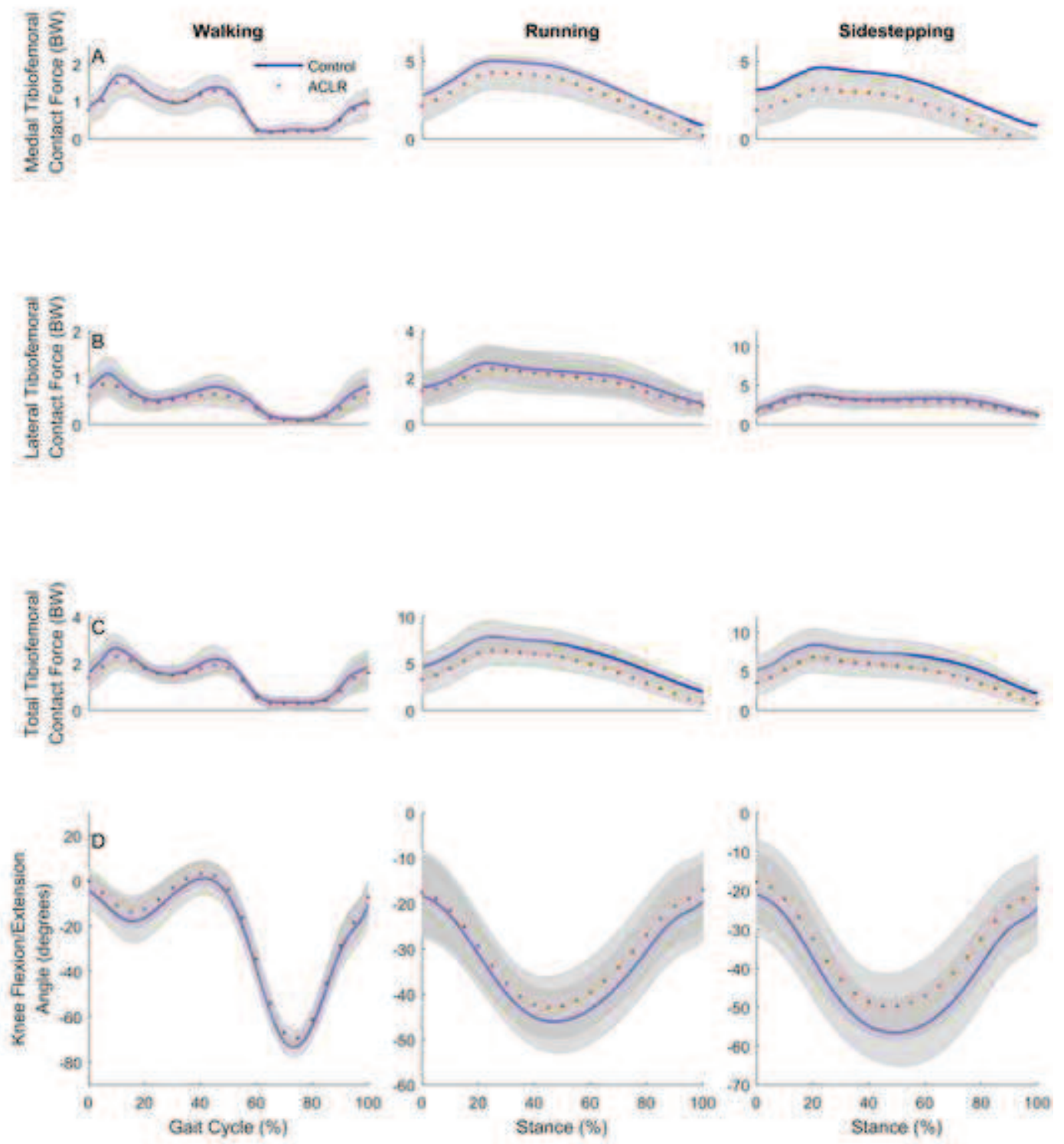


Figure 3. Contributions to medial contact force

[Click here to download Figure ctrACLRMuscExtCont2MedLoad.tif](#)

